

Article

An Underwater Wet-Mateable Electrical Connector with Dual-Bladder Pressure-Balanced Oil-Filled (PBOF) Technology

Wentao Song^{1,2,3}, Cuibo Yang⁴, Weicheng Cui^{2,3,*} , Changhui Song^{2,3,5}, Ping Yang^{2,3}, Jin Hong⁴, Yi Lei⁴, Qimeng Liu^{1,2,3}  and Zhenhua Wang^{1,2,3} 

¹ Zhejiang University–Westlake University Joint PhD Program, Zhejiang University, Hangzhou 310058, China

² Key Laboratory of Coastal Environment and Resources of Zhejiang Province, School of Engineering, Westlake University, Hangzhou 310024, China

³ Institute of Advanced Technology, Westlake Institute for Advanced Study, Hangzhou 310024, China

⁴ Shanghai Kingboom Transmission Technology Co., Ltd., Shanghai 201806, China

⁵ Zhejiang Nektron Intelligent Technology Co., Ltd., Hangzhou 310024, China

* Correspondence: weichengcui@westlake.edu.cn

Abstract: Underwater wet-mateable connectors have been widely used to reduce the cost and the time of installation, maintenance and reconfiguration in many fields, such as the oil and gas (O&G) industry, offshore renewable energy (ORE), and undersea observatories. In the past few years, the authors' group has made some efforts in developing wet-mateable connectors. This paper presents a methodology for designing and testing a wet-mateable electrical connector. First, an innovative wet-mateable electrical connector with dual-bladder pressure-balanced oil-filled (PBOF) technology is proposed. Second, the generalized equations of differential pressure are derived. Then, a procedure of thermal-electric-structure (TES) coupling simulation is proposed, and a series of finite element analysis (FEA) involving coupled multi-field problems is conducted, including thermal-electric coupling analysis, static structural analysis, and dynamic analysis. Finally, a prototype of the proposed connector is developed successfully, and its electrical performance is verified by the online test in a hydrostatic pressure environment with an ocean depth of 3000 m, which has reached the leading level in China. This paper is the first discloser on wet-mateable connectors in the aspects of design, theory, simulation and testing, which might be helpful to many ocean scientists in developing countries who are technically blocked or could not afford the high cost.

Keywords: wet-mateable; electrical connector; pressure-balanced oil-filled (PBOF); coupled multi-field; prototype test



Citation: Song, W.; Yang, C.; Cui, W.; Song, C.; Yang, P.; Hong, J.; Lei, Y.; Liu, Q.; Wang, Z. An Underwater Wet-Mateable Electrical Connector with Dual-Bladder Pressure-Balanced Oil-Filled (PBOF) Technology. *J. Mar. Sci. Eng.* **2023**, *11*, 156. <https://doi.org/10.3390/jmse11010156>

Academic Editor: Spyros Hirdaris

Received: 27 November 2022

Revised: 13 December 2022

Accepted: 5 January 2023

Published: 9 January 2023



Copyright: © 2023 by the authors. Licensee MDPI, Basel, Switzerland. This article is an open access article distributed under the terms and conditions of the Creative Commons Attribution (CC BY) license (<https://creativecommons.org/licenses/by/4.0/>).

1. Introduction

Energy demand drove the industrial revolution in the 1800s, and it may drive another new round of industrial revolution in the 21st century [1]. The ocean has abundant resources (e.g., minerals, renewable energy, genes, space, etc.), which are essential for human beings to achieve sustainable development [2]. However, we have just explored less than 20% of the ocean, and only 5% in detail [3,4]. Although submersibles are the main working force for the research fleet, various deep-sea equipment deployed in the oil and gas (O&G) industry, offshore renewable energy (ORE), and undersea observatories are also fundamental to the effective exploration and utilization of the ocean world and marine resources.

Underwater wet-mateable connectors can be mated and de-mated under the sea, they have been extensively used in the above fields to reduce the cost and the time of installation, maintenance and reconfiguration [5]. The O&G industry is the biggest consumer of wet-mateable connectors. With the increase in the depth of exploitation, wet-mateable electrical connectors that can be used in a harsh environment with high ocean pressure and submarine seismic risks are the main demand. As is experienced in the O&G exploration and production, most of the needed wet-mateable connectors with high voltage rates (less

than 12 kV) should be operated at depths of up to 3000 m [6]. ORE farms also need a large number of wet-mateable electrical connectors. With the development of technologies of offshore wind energy, tidal stream, and ocean current energy, the requirement for wet-mateable connectors with high power is also increasing [7,8]. In this field, the voltage rate of the required wet-mateable connectors ranges from 1 kV to 33 kV, while their depth rate is only up to 100 m [6,8]. The application of wet-mateable connectors in ORE farms has the advantage of allowing the transformer to be lifted out of the water with no need to lift the long and heavy cable [9]. Another important application field of wet-mateable connectors is undersea observatories, for example, the Astronomy with a Neutrino Telescope and Abyss environmental RESearch (ANTARES) project [10] and the next-generation neutrino telescopes KM3NeT [11]. Figure 1 presents a schematic of the complete link between the string power module/string control module (SPM/SCM) and the junction box in ANTARES. Whereas the mounting of the jumpers is performed on shore, the completion of the wet-mate connection can be realized by a remotely operated vehicle (ROV) [10]. So, wet-mateable connectors can provide an effective solution to the expansion and networking of undersea observatories [3].

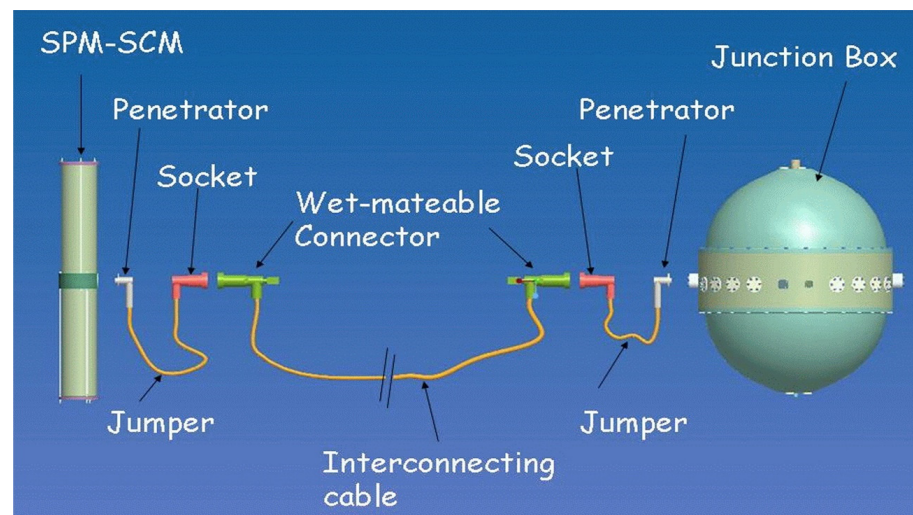


Figure 1. A schematic of the complete link between the string power module/string control module (SPM/SCM) and the junction box in ANTARES [10].

However, only a few developed countries can produce wet-mateable connectors worldwide. The key technologies are mostly confidential and protected by patents, so there are few published papers on this topic, which makes wet-mateable connectors become one of the bottleneck techniques in China [3,5]. Conceivably, the market price of wet-mateable connectors is very expensive. For example, the cost of a wet-mateable hybrid connector rated at 11 kV is expected to be in the range of £250 k/unit [8], and even low-spec products may cost as much as £20 k/unit [6]. Today, the top manufacturers of wet-mateable connectors include SEACON, MacArtney Group, Teledyne ODI, Siemens Energy, and so on. Each vendor has its own unique technology [3,7,8].

In the past few years, the authors' group has made some efforts in developing wet-mateable connectors. In 2021, Song and Cui [3] gave a very detailed overview of wet-mateable connectors and proposed the concept of functional units to present a better understanding of the key technologies involving electrical/optical connection, pressure-balanced oil-filled (PBOF), penetrable self-sealing, automatic interlocking/docking (AID) and so on. Readers can refer to the literature [3] for details. Among these key technologies, PBOF is the most essential for wet-mateable connectors, which can eliminate the differential pressure of connectors, making the wet-mate possible [3,5,7,12]. In 2022, Song et al. [5] presented a very detailed investigation of PBOF technology and developed the core compo-

ment used in wet-mateable connectors: a rubber-made resilient bladder [5]. Compared to commercial off-the-shelf (COTS) products, this resilient bladder has a simple structure and lower cost, and it is more suitable for mass production. The results of the tests verified that the depth rate of the new bladder is greater than 6500 m. In the next step, the authors' group aims to develop a wet-mateable electrical connector. The simulation technique involving a coupled multi-field problem is a proven way to save the cost and the time of research and development (R&D) [13]. The finite element method (FEM) can be easily adapted to constitutive equations of different physical fields [14]. So, finite element analysis (FEA) will play a very important role in this work.

In the future, the next-generation submersible will be more inspired by fish in nature. Compared with traditional submersibles, bio-inspired fish robots have the advantages of high efficiency, high maneuverability, low noise, and so on [15,16]. Meanwhile, the next-generation submersible will have more functions, such as underwater charging. If submersibles land on an underwater docking station, the power transfer can be achieved by using wet-mateable connectors [17,18]. Foreseeably, wet-mateable connectors must have a bright application prospect.

In this paper, the authors proposed an underwater wet-mateable electrical connector with dual-bladder PBOF technology. First, the generalized differential pressure equations of dual-bladder PBOF technology are derived. Second, a procedure of coupled multi-field simulation for wet-mateable electrical connectors is proposed. Then, a series of FEA is conducted, including thermal-electric coupling analysis, static structural analysis, and dynamic analysis. Finally, a prototype of the proposed connector is developed successfully, and its electrical performance is verified by a series of tests. The technical level of this prototype has reached the leading position in China. This paper might be the first disclosure on wet-mateable connectors in the aspects of design, theory, simulation, and testing, which might be helpful to many ocean scientists in developing countries who are technically blocked or could not afford the high cost.

2. Design and Theory

2.1. Overall Design

The main specifications of the proposed wet-mateable electrical connector are listed in Table 1. Considering the current demands in the O&G industry and undersea observatories in China, the operating depth of wet-mateable connectors will not exceed 3000 m in the next five years. Other specifications mainly refer to some first-class COTS products, such as SECAON HydraElectric, Nautilus™ WM1.7-30, and Siemens DigiTRON.

Table 1. Main specifications of the proposed wet-mateable electrical connector.

Number of Contacts	Depth Rating	Contact Resistance	Insulation Resistance	Operating Current	Operating Voltage
4	3000 m	≤5 mΩ	≥10 GΩ	≤30 A	≤1.5 kV DC

Figure 2 presents a schematic of the proposed connector which consists of two parts: the plug unit and the receptacle unit. The dual-bladder PBOF technology is introduced to improve reliability, and its core components are two kinds of resilient bladder (parts 12 and 13). The shuttle pin design is used in electric connections to achieve penetrable self-sealing, and its core component is a moveable stopper (part 11) and the contact pin with an insulating layer (part 3). The proposed connector also has the AID technology which can facilitate ROVs to operate under the sea, and its core component is a latching member (part 4). Compared to available products, the proposed connector is a smaller-sized one, whose maximum radial dimension is less than 100 mm and the axial dimension in the mated state is less than 210 mm. The key technologies of the proposed connector are patented by China National Intellectual Property Administration [19].

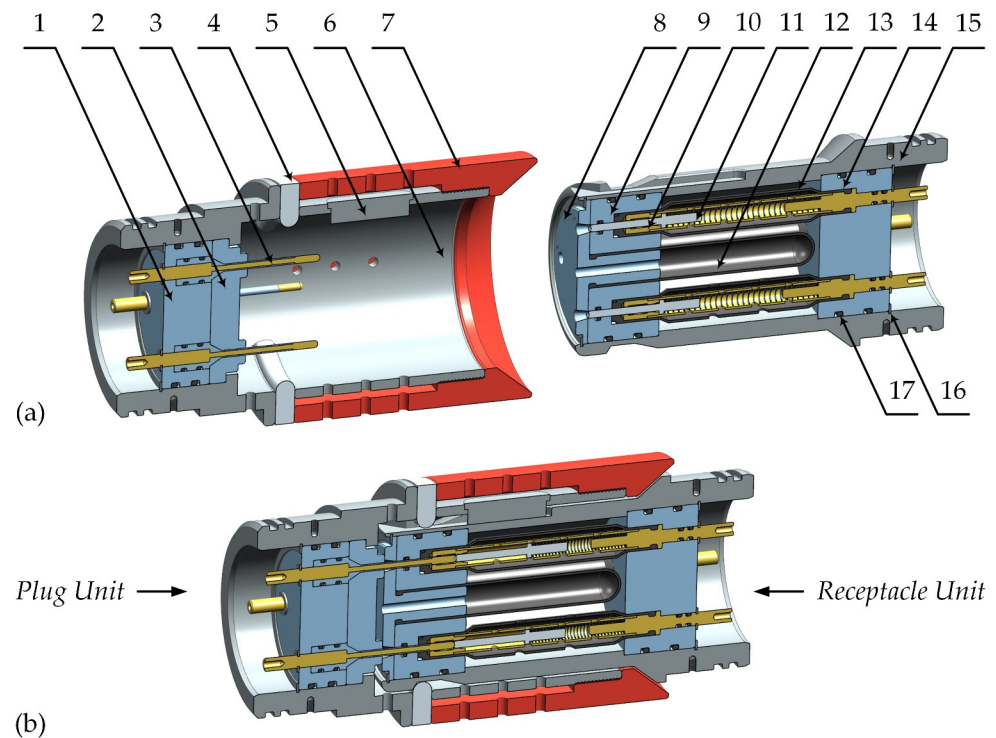


Figure 2. A schematic illustration of (a) the de-mated state and (b) the fully mated state of the proposed wet-mateable electrical connector: 1-plug pedestal; 2-plug orifice plate; 3-contact pin with an insulating layer; 4-latching member; 5-aligning key; 6-plug shell; 7-dust cap; 8-receptacle orifice plate; 9-receptacle front pedestal; 10- electric connection; 11-moveable stopper; 12-primary resilient bladder; 13-secondary resilient bladder; 14-receptacle rear pedestal; 15-receptacle shell; 16-retaining ring; 17-O-ring.

2.2. PBOF Design

PBOF technology can provide a small mating/de-mating force and sealing pressure with better reliability. Thus, the general O-ring sealing design can be used in the proposed connector. Figure 3 presents a schematic of the dual-bladder PBOF technology used in the proposed connector. The primary oil chamber is formed outside of the primary resilient bladder, while the independent secondary oil chambers are formed inside each secondary bladder. The oil chambers are all filled with the dielectric oil by a custom hypodermic tube of a syringe which can be inserted through each passageway of the moveable stopper. In the ocean, the primary bladder separates seawater and filled-oil. The ocean pressure can be transmitted to the oil in the primary oil chamber first and then to that in the secondary oil chamber, so an internal pressure is produced to balance the ocean pressure.

In particular, to fill the primary oil chamber, one secondary bladder must be punched through with holes to connect the primary oil chamber and its secondary oil chamber. So, this electrical channel protected by only one bladder can be used for unimportant circuits or ground terminals. The frequently used filled oil is the XIAMETER™ PMX-200 silicon fluid (previously known as DC 200) produced by Dow Corning, which has good water-repellency, lubrication, and dielectric property [3]. Fluorosilicone rubber is preferred to make such bladders that shall not react with silicone oil and seawater.

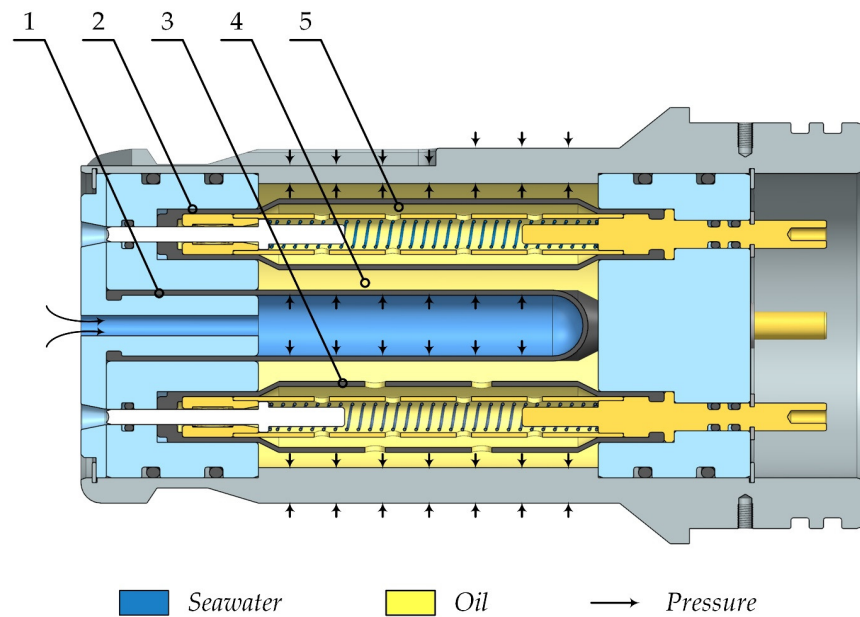


Figure 3. A schematic illustration of the dual-bladder PBOF technology used in the proposed wet-mateable electrical connector: 1-primary resilient bladder; 2-secondary resilient bladder; 3-secondary resilient bladder with through-holes; 4-primary oil chamber; 5-secondary oil chamber.

2.3. PBOF Theory

Due to the compressibility of oil, a differential pressure between the ambient pressure and the oil pressure will arise, which is a very important indicator of PBOF technology. The authors' group has studied this problem systematically and the results are presented in a previous publication [5]. On this basis, this paper further gives the generalized differential pressure equations of the dual-bladder PBOF technology. For the proposed connector, the differential pressure of the primary resilient bladder can be determined by the following equations.

$$C_{11} \cdot \Delta P_1^2 + C_{21} \cdot \Delta P_1 + C_{31} = 0 \tag{1}$$

$$\begin{cases} C_{11} = \frac{(2-\mu_1)^2 R_1^4}{2E_1^2 \delta_1^2} \left(\frac{L_1}{2} - 2k_{11} + k_{21} \right) \\ C_{21} = \frac{2(2-\mu_1)R_1^3}{E_1 \delta_1} \left(\frac{L_1}{2} - k_{11} \right) + \frac{R_0^2 L_0 - (R_1 - \delta_1)^2 L_1}{E_B} \\ C_{31} = -\frac{R_0^2 L_0 - (R_1 - \delta_1)^2 L_1}{E_B} \cdot P \end{cases} \tag{2}$$

$$\begin{cases} k_{11} = \frac{1}{\beta_1} \left(1 - e^{-\frac{\beta_1 L_1}{2}} \cos \frac{\beta_1 L_1}{2} \right) \\ k_{21} = \frac{1}{4\beta_1} \left[3 - e^{-\beta_1 L_1} (2 + \sin \beta_1 L_1 + \cos \beta_1 L_1) \right] \\ \beta_1 = \frac{\sqrt[4]{3(1-\mu_1^2)}}{\sqrt{R_1 \delta_1}} \end{cases} \tag{3}$$

where

P is the ocean pressure, in the unit of MPa;

ΔP_1 is the differential pressure of the primary resilient bladder, in the unit of MPa;

E_1 is the apparent elastic modulus of the primary resilient bladder, in the unit of MPa;

E_B is the bulk modulus of the filled-oil, in the unit of MPa;

L_0 is the length of the primary oil chamber, in the unit of mm;

L_1 is the length of the primary resilient bladder, in the unit of mm;

R_0 is the internal radius of the primary oil chamber, in the unit of mm;

R_1 is the external radius of the primary resilient bladder, in the unit of mm;

δ_1 is the thickness of the primary resilient bladder, in the unit of mm;
 μ_1 is the Poisson's ratio of the primary resilient bladder.

Similarly, the differential pressure equation of the secondary resilient bladder can be obtained by the following equations.

$$C_{12} \cdot \Delta P_2^2 + C_{22} \cdot \Delta P_2 + C_{32} = 0 \tag{4}$$

$$\begin{cases} C_{12} = \frac{(2-\mu_2)^2 R_2^4}{2E_2^2 \delta_2^2} \left(\frac{L_2}{2} - 2k_{12} + k_{22} \right) \\ C_{22} = \frac{2(2-\mu_2)R_2^3}{E_2 \delta_2} \left(\frac{L_2}{2} - k_{12} \right) + \frac{R_0^2 L_0 - (R_2 - \delta_2)^2 L_2}{E_B} \\ C_{32} = -\frac{R_0^2 L_0 - (R_2 - \delta_2)^2 L_2}{E_B} \cdot P \end{cases} \tag{5}$$

$$\begin{cases} k_{12} = \frac{1}{\beta_2} \left(1 - e^{-\frac{\beta_2 L_2}{2}} \cos \frac{\beta_2 L_2}{2} \right) \\ k_{22} = \frac{1}{4\beta_2} \left[3 - e^{-\beta_2 L_2} (2 + \sin \beta_2 L_2 + \cos \beta_2 L_2) \right] \\ \beta_2 = \frac{\sqrt[4]{3(1-\mu_2^2)}}{\sqrt{R_2 \delta_2}} \end{cases} \tag{6}$$

where

ΔP_2 is the differential pressure of the secondary resilient bladder, in the unit of MPa;
 E_2 is the apparent elastic modulus of the secondary resilient bladder, in the unit of MPa;

L_2 is the length of the secondary resilient bladder, in the unit of mm;

R_2 is the external radius of the secondary resilient bladder, in the unit of mm;

δ_2 is the thickness of the secondary resilient bladder, in the unit of mm;

μ_2 is the Poisson's ratio of the secondary resilient bladder.

Therefore, the total differential pressure of the proposed connector is as follows:

$$\Delta P = \Delta P_1 + \Delta P_2 \tag{7}$$

For the proposed connector, we have $R_0 = 28$ mm, $L_0 = 67$ mm, and $E_B = 1034$ MPa. For two resilient bladders, we have $E_1 = E_2 = 22$ MPa, $R_1 = R_2 = 7$ mm, $\delta_1 = \delta_2 = 1$ mm, $\mu_1 = \mu_2 = 0.5$, $L_1 = 65$ mm, and $L_2 = 67$ mm. Then, the differential pressures of the proposed connector can be determined. Figure 4 presents a three-dimensional (3D) view of two bladders, as well as the theoretical results of their differential pressures. The results are given as follows:

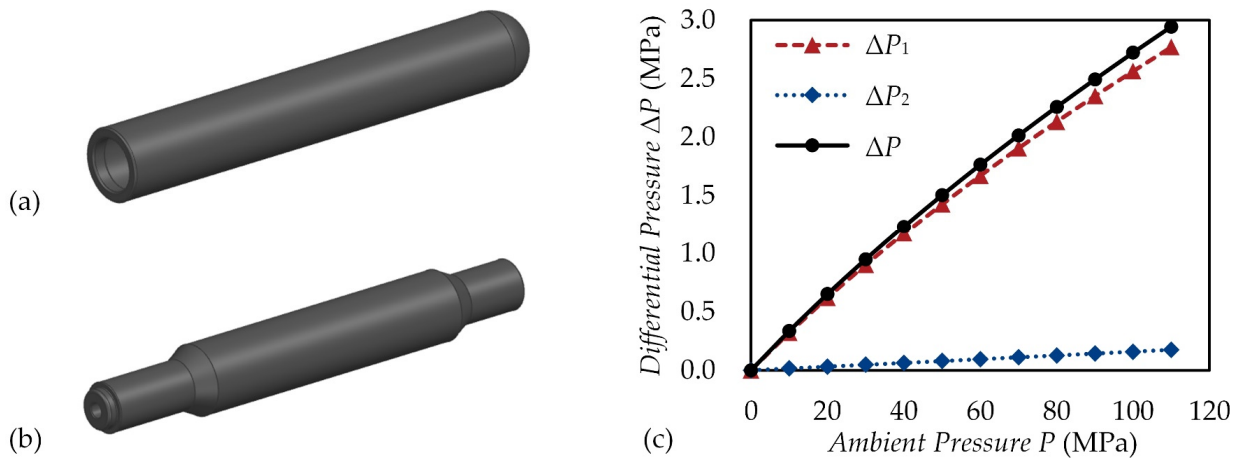


Figure 4. A 3D view of (a) the primary resilient bladder and (b) the secondary resilient bladder, and (c) the change curves of the differential pressures in the proposed wet-mateable electrical connector.

(1) The total differential pressure is mainly determined by the primary bladder, which is almost less than 3.5% of the ocean pressure.

(2) The differential pressure of the secondary bladder is much smaller than that of the primary bladder. This reminds us that the differential pressure provided by the bladder under the action of internal pressure is much larger than that provided by such a bladder with a similar dimension but under the action of external pressure.

(3) Although the dual-bladder PBOF technology can improve reliability, it may also increase the total differential pressure. Nevertheless, due to the pressure-balanced mode of the secondary bladder, there is only a slight impact on the performance.

2.4. Shuttle Pin Design

The shuttle pin design can provide the sealing performance in the dynamic process of mating and de-mating, which belongs to a penetrable seal-sealing [3,20]. As is depicted in Figure 5, when the contact pin is inserted into the electric socket, it will push the moveable stopper inside and make full contact with the crown spring. Thus, the current will flow through the pin to the socket, and then to the conductive sleeve and the conductive shaft in turn. When the pin is de-mated, the stopper will be followed by the pin closely under the action of the spring force. Therefore, the sealing performance can always be guaranteed by this penetrable self-sealing design.

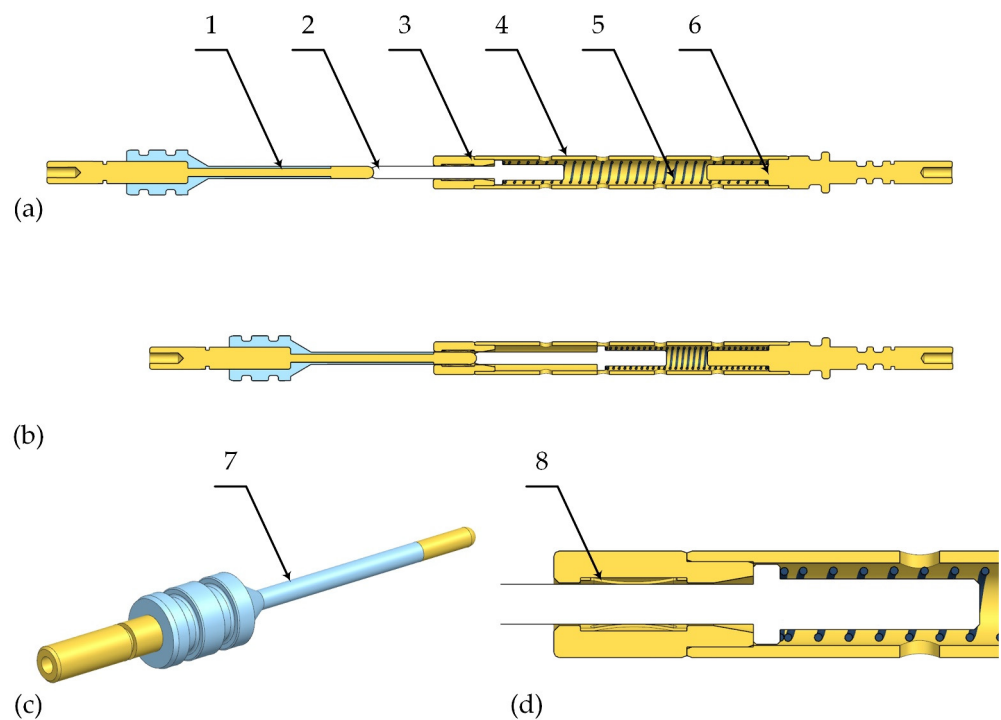


Figure 5. A schematic illustration of the shuttle pin design in (a) the disconnecting state and (b) the connecting state, and the detail views of (c) the contact pin and (d) the electric socket: 1-contact pin; 2-moveable stopper; 3-electric socket; 4-conductive sleeve; 5-spring; 6-conductive shaft; 7-insulating layer; 8-crown spring.

The shuttle pin design involves the following essential components and subtle design skills:

(1) The moveable stopper must be an insulating part, which is made of polyetheretherketone (PEEK). The diameter of the stopper is only 3 mm, which almost reaches the limit of commercial off-the-shelf (COTS) products. The stopper’s small size brings great challenges to the manufacturing and the penetrable self-sealing. Therefore, it presents one of the most difficult challenges in developing wet-mateable electrical connectors.

(2) The contact pin, as shown in Figure 5c, has an insulating layer made of PEEK to prevent seawater from contacting the conductor after the intrusion, which is almost as expensive as the resilient bladder due to the difficulty of processing.

(3) The maximum deformation of the spring should satisfy the hypodermic tube of the syringe and can reach the position of oil-filling. Additionally, the authors recommend using the piano-wire spring which has good performance in strength and fatigue resistance.

(4) According to the requirement of the maximum operating current, the standard parts can be selected for the crown spring, which is usually made of beryllium copper. The other conductive components can be made of copper alloys, such as brass or lead brass. Moreover, gold plating can be used on the electrical contact surface to decrease contact resistance.

(5) An easily occurred and fatal failure mode of the shuttle pin design is that the moveable stopper cannot eject to the original position after de-mating. To avoid this, the end of the stopper and the end of the fitted hole in the electric socket are both designed as cone types, which are shown in Figure 5d. This skill can also increase allowable fit tolerances to decrease the cost of manufacturing.

(6) It is worth noting that PEEK plastic is a very important dielectric material used in wet-mateable electrical connectors, which has good insulating properties in harsh environments under the sea. Also, PEEK is a self-lubricating material with higher tensile and yield strength and excellent fatigue resistance [3].

3. Finite Element Analysis

3.1. Coupled Multi-Field Simulation

Due to the Joule heating effect, wet-mateable electrical connectors will inevitably generate heat when they transfer electricity. However, the excessive temperature will reduce the elasticity of electric contact and soften the insulating material, resulting in the failure of connection and insulation. Moreover, thermal stress may also cause a fatal effect on the reliability of the structure. For example, if high stress produces a large deformation of the moveable stopper, the function of the penetrable self-sealing will be totally lost. Therefore, the coupled multi-field simulation is indispensable for the development of wet-mateable electrical connectors.

Here, the basic equations of thermal-electric coupling are given as follows. Equations (8) and (9) are derived from the heat flow equation and the charge continuity equation respectively, and Equation (10) is the constitutive equation for the dielectric medium [14,21].

$$\rho C \frac{\partial T}{\partial t} + \nabla \cdot ([\Pi] \cdot J) - \nabla \cdot ([\lambda] \cdot \nabla T) = \dot{q} \tag{8}$$

$$\nabla \cdot \left([\varepsilon] \cdot \nabla \frac{\partial \varphi}{\partial t} \right) + \nabla \cdot ([\sigma] \cdot [\alpha] \cdot \nabla T) + \nabla \cdot ([\sigma] \cdot \nabla \varphi) = 0 \tag{9}$$

$$D = [\varepsilon] \cdot E \tag{10}$$

where

C is the specific heat capacity, in the unit of $J/(kg \cdot ^\circ C)$;

T is the absolute temperature, in the unit of $^\circ C$;

\dot{q} is the heat generation rate, in the unit of W/m^3 ;

ρ is the density, in the unit of kg/m^3 ;

D is the electric flux density vector, in the unit of C/m^2 ;

E is the electric field intensity vector, in the unit of V/m ;

J is the electric current density vector, in the unit of A/m^2 ;

$[\Pi]$ is the Peltier coefficient matrix, $[\Pi] = T \cdot [\alpha]$, in the unit of V ;

$[\alpha]$ is the Seebeck coefficient matrix, in the unit of $V/^\circ C$;

$[\varepsilon]$ is the dielectric permittivity matrix, in the unit of F/m ;

$[\lambda]$ is the thermal conductivity matrix, in the unit of $W/m \cdot ^\circ C$;

$[\sigma]$ is the electrical conductivity matrix, in the unit of S/m .

By applying the Galerkin FEM procedure to the above-derived coupled equations, the thermoelectric finite element equations can be obtained as follows [14,21]:

$$\begin{bmatrix} C^{TT} & 0 \\ 0 & C^{\varphi\varphi} \end{bmatrix} \begin{pmatrix} \dot{T}_e \\ \dot{\varphi}_e \end{pmatrix} + \begin{bmatrix} K^{TT} & 0 \\ K^{\varphi T} & K^{\varphi\varphi} \end{bmatrix} \begin{pmatrix} T_e \\ \varphi_e \end{pmatrix} = \begin{pmatrix} Q \\ I \end{pmatrix} \quad (11)$$

where

- C^{TT} is the thermal damping matrix;
- $C^{\varphi\varphi}$ is the dielectric damping matrix;
- K^{TT} is the thermal stiffness matrix;
- $K^{\varphi T}$ is the Seebeck stiffness matrix;
- $K^{\varphi\varphi}$ is the electric stiffness matrix;
- I is the electric current load vector;
- Q is the combined heat load vector;
- T_e is the nodal temperature vector;
- φ_e is the nodal electric potential vector.

As is depicted in Figure 6, the authors proposed a procedure of thermal-electric-structure (TES) coupling simulation for wet-mateable electrical connectors, which can be achieved by FEM based on ANSYS software. The interface of ANSYS Workbench can easily realize coupled-field analysis. First, an FEA model involving thermal-electric coupling is proposed to verify the thermoelectricity of the above-designed connector. Second, the obtained temperature distribution should be transferred to the static structural FEA model. Then, the thermal stress distribution can be determined to verify the reliability of the structure. Furthermore, the pre-stress in the structure cannot be ignored in dynamic analysis. Thus, thermal stress should be transferred to the FEA model of modal analysis. Only in this step can accurate dynamic analyses be done. The simulation results of the proposed connector will be presented and discussed next. All the material specifications used in the FEA models are listed in Table 2, which are from ANSYS GRANTA Materials Database.

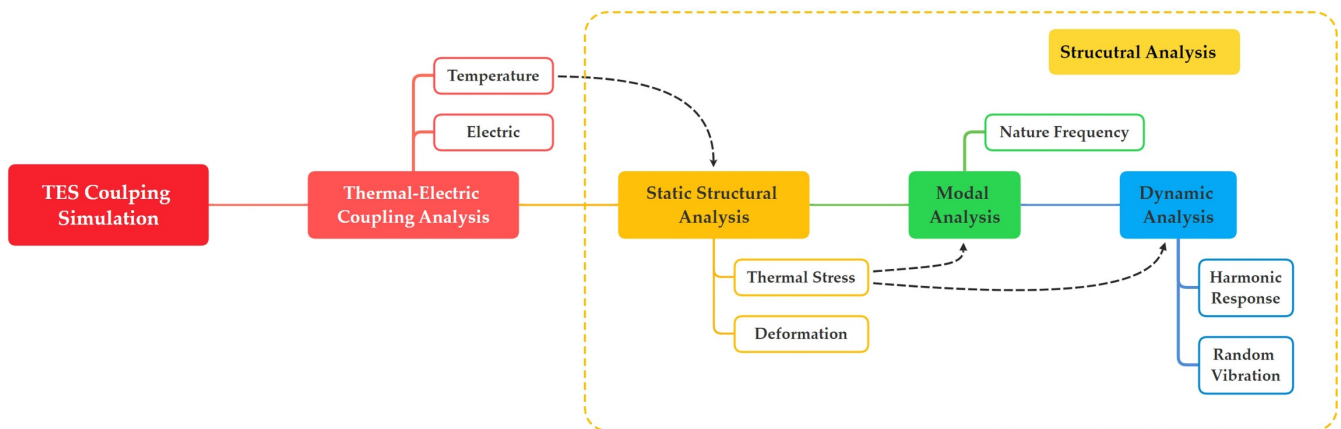


Figure 6. A schematic illustration of the TES coupling simulation for wet-mateable electrical connectors.

Table 2. Material specifications of the proposed wet-mateable electrical connector.

Property	Material	Copper Alloy	PEEK Plastic	Fluorosilicone Rubber *	Stainless Steel
Density (kg/m ³)		8940	1310	1120	7900
Isotropic Thermal Conductivity (W/m·°C)		394	0.25	0.245	15
Isotropic Resistivity (S/m)		1.72×10^{-8}	9.95×10^{13}	1.22×10^{12}	7.07×10^{-7}
Coefficient of Thermal Expansion (1/°C)		1.70×10^{-5}	5.48×10^{-5}	2.74×10^{-4}	1.70×10^{-5}
Young’s Modulus (GPa)		131	3.85	-	198
Poisson’s Ratio		0.345	0.4	-	0.27
Yield Strength (MPa)		247	90.9	8.97	243
Tensile Strength (MPa)		320	96.3	8.97	546

* The hyper-elastic of the fluorosilicone rubber is described by Mooney-Rivlin model with the constants $C_{10} = 2.59 \times 10^5$ Pa and $C_{01} = 6.5 \times 10^4$ Pa.

3.2. Thermal-Electric Coupling Analysis

A thermal-electric coupling FEA model is proposed based on ANSYS Mechanical, and the corresponding boundary conditions include the following aspects:

- (1) The current I is applied to the end-face of the contact pin (here $I = 40$ A). The voltage U of the end-face of the conductive shaft is set to be zero ($U = 0$).
- (2) Due to the existence of contact resistance R_{contact} , a heat flow Q_{HF} is applied on the surface of the electric contact (here, $Q_{\text{HF}} = I^2 \cdot R_{\text{contact}} = 3.2$ W).
- (3) According to different conditions of the environment, the convective film coefficient $h_{\text{convective}}$ is set on the corresponding heat dissipation surface.

To begin with, Figure 7 presents the temperature distribution of the electric contact with PBOF technology, as well as corresponding boundary conditions. The results are shown as follows:

- (1) The maximum temperature of the electric contact in Figure 7a is about 74.61 °C, while it is decreased by 2.85% to about 72.48 °C in Figure 7b. The maximum temperature of the crown spring in Figure 7a is about 69.29 °C, while it is decreased by 3.09% to about 67.15 °C in Figure 7b.

- (2) Due to the higher convective film coefficient of oil, PBOF technology can improve the heat dissipation capability of the electric contact. Importantly, because the use of the secondary resilient bladder increases the area of dissipation, the dual-bladder PBOF technology can further reduce thermal power by about 3%.

Figure 8 further gives the temperature distribution of the whole connector in terrestrial and underwater environments respectively, as well as the corresponding boundary conditions. Figure 9 presents the electric field distribution of some insulating components in an underwater environment, as well as the corresponding maximum intensity E_{max} . The results are shown as follows:

- (1) The maximum temperature of the proposed connector in a terrestrial environment is about 53.92 °C, while it is decreased by about 35.17% to 34.98 °C in the underwater environment. The maximum temperature in both cases appears on the contact pin.

- (2) The ambient temperature under the sea is much lower than the terrestrial temperature. Also, the convective film coefficient of seawater is much larger than that of air. This allows better heat dissipation of wet-mateable electrical connectors in the operating condition, which can further be improved by the dual-bladder PBOF technology. As a result, the overcurrent capacity of the proposed connector will exceed the rated current of the crown spring.

- (3) The receptacle front pedestal has the strongest electric field with an intensity of 21.8 kV/mm, which almost reaches the breakdown field of PEEK. The electric field intensities of other insulating components are much smaller. The analysis of thermoelectric performance further confirms that the maximum operating current of the proposed connector can reach 40 A.

To this extent, the thermal-electric coupling analysis further reveals a characteristic of wet-mateable electrical connectors, that is, the overcurrent capacity can be enhanced by the underwater environment and PBOF technology. Therefore, we revised the maximum

operating current in Table 1 as follows: 30 A in dry conditions and 40 A under the sea. Moreover, the glass fibre-reinforced PEEK can be used to provide better resistance to dielectric breakdown.

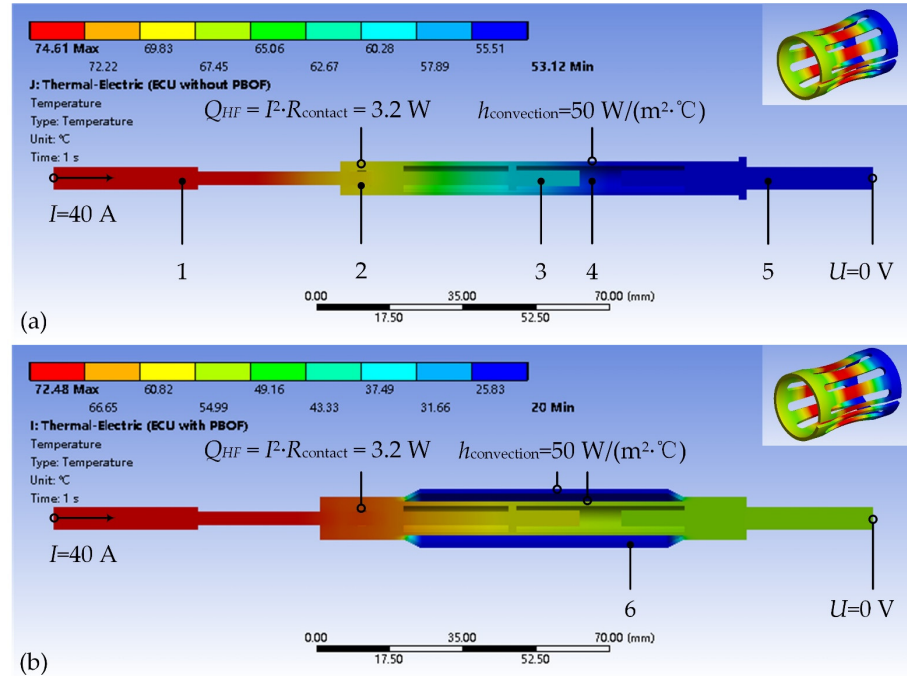


Figure 7. The temperature distribution of the electric contact with (a) PBOF technology and (b) dual-bladder PBOF technology: 1-contact pin; 2-electric socket; 3-moveable stopper; 4-conductive sleeve; 5-conductive shaft; 6-secondary resilient bladder.

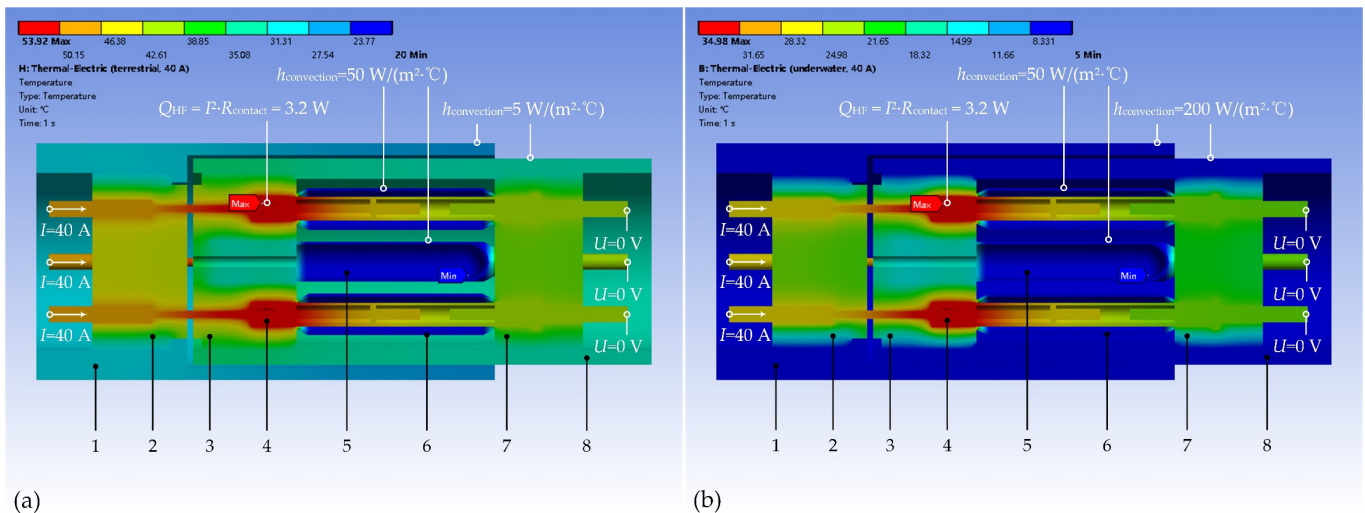


Figure 8. The temperature distribution of the proposed wet-mateable electrical connector in (a) terrestrial environment (the ambient temperature is 20 °C) and (b) underwater environment (the ambient temperature is 5 °C): 1-plug shell; 2-plug pedestal; 3-receptacle front pedestal; 4-electric contact; 5-primary resilient bladder; 6-secondary resilient bladder; 7-receptacle rear pedestal; 8-receptacle shell.

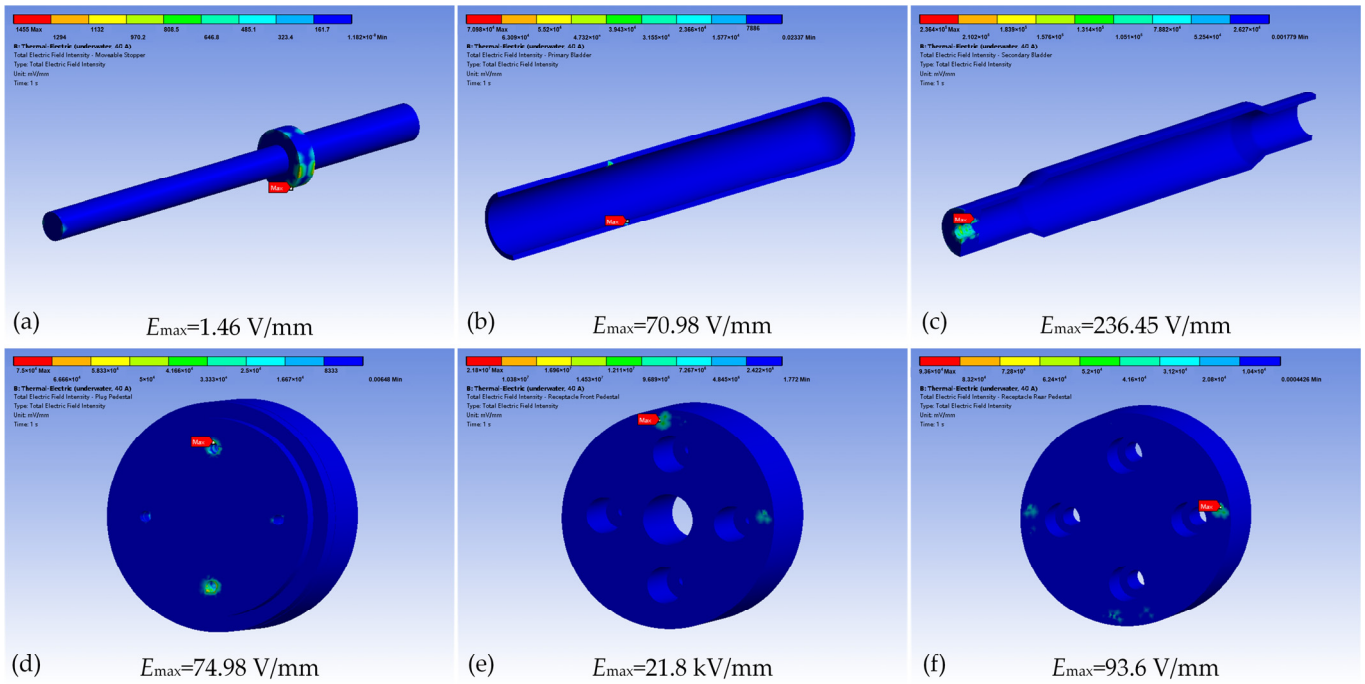


Figure 9. The voltage distribution of the main insulating components in an underwater environment (the ambient temperature is 5 °C): (a) moveable stopper, (b) primary resilient bladder, (c) secondary resilient bladder, (d) plug pedestal, (e) receptacle front pedestal, and (f) receptacle rear pedestal.

3.3. Static Structural Analysis

A static structural FEA model based on ANSYS Mechanical is proposed. The obtained temperature distribution from the thermal-electric analysis is coupled with this FEA model to calculate the thermal stress. Figure 10 presents the stress distribution of some core components, as well as the corresponding maximum stress σ_{max} . The results are shown as follows:

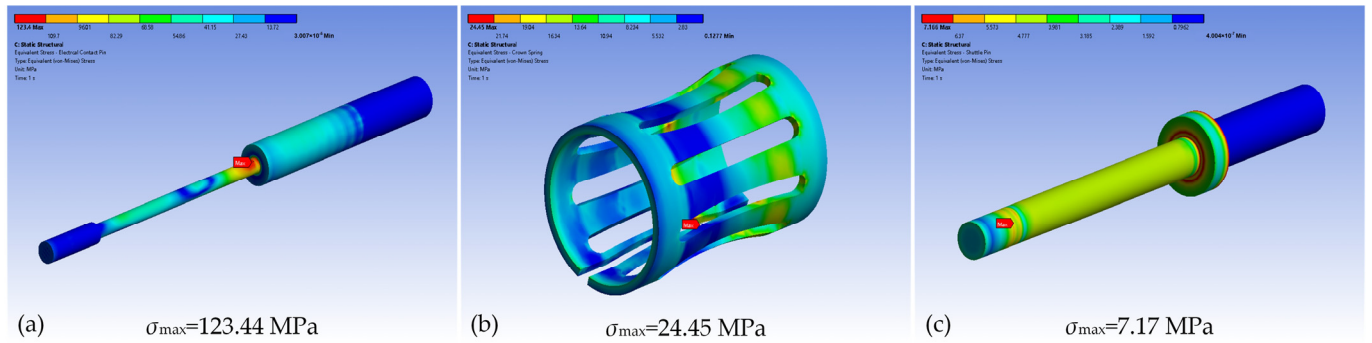


Figure 10. The thermal stress distribution of some core components of the proposed wet-mateable electrical connector: (a) contact pin, (b) crown spring, and (c) moveable stopper.

(1) The components having large deformation are the resilient bladders, and the maximum deformation is about 0.97 mm which has no influence on the reliability of the structure. The deformation of the moveable stopper is just about 0.02 mm at maximum, which has no effect on the function of the shuttle pin design.

(2) The components having large thermal stress are the contact pins, and the maximum equivalent stress is about 123.44 MPa which is less than the yield stress of copper alloy. The equivalent stress of the crown spring is about 24.45 Mpa in maximum, which has no effect on its elasticity. The thermal stress of the moveable stopper is much smaller.

In this subsection, a static structural FEA model of the AID technology is also proposed to verify the performance and provide guidance for the selection of the latching member’s material. Figure 11 presents the mating process in the simulation, and Figure 12 gives the change curves of the mating/de-mating force and the equivalent stress of the latching member. The results are given as follows:

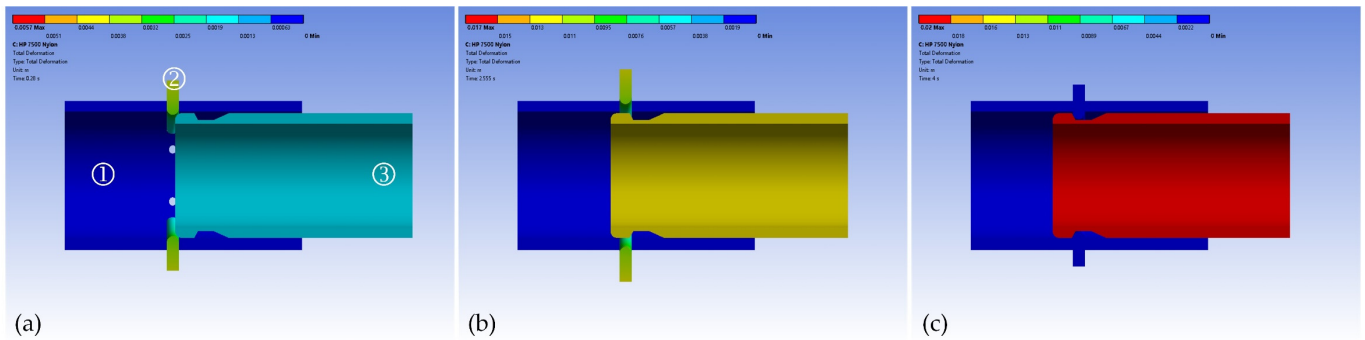


Figure 11. The mating process of the latching mechanism in the simulation: (a) the receptacle (part 3) starts engaging with the plug (part 1), (b) the receptacle is made the maximum engagement with the latching member (part 2), and (c) the plug and the receptacle are fully mated and interlocked by the latching member.

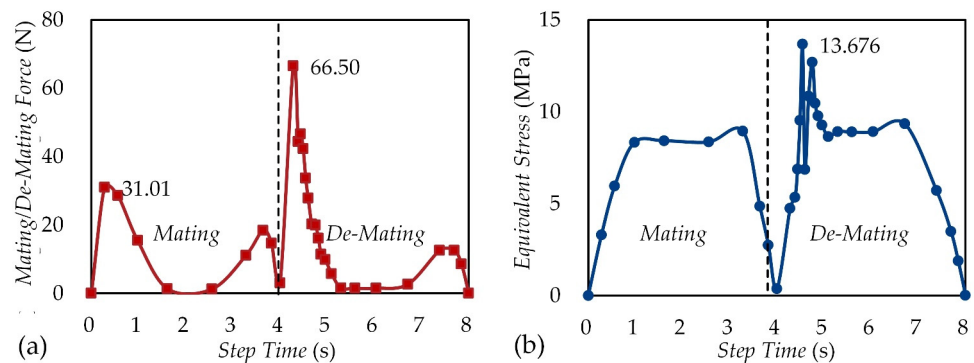


Figure 12. The change curves of (a) the mating/de-mating force and (b) the equivalent stress of the latching member.

(1) The latching member must have the appropriate elastic constants. If the Young’s modulus of the material is too small, it cannot provide enough locking force, while if Young’s modulus is too large, the mating force will be increased. According to the simulation results, the material with Young’s modulus of about 70 MPa is the ideal material for the latching member.

(2) The de-mating force of the proposed AID technology is about 66.50 N, while the mating force is about 31.01 N. The de-mating force should be appropriately larger than the mating force, which can achieve easy docking and reliable interlocking of the wet-mateable connectors.

3.4. Dynamic Analysis

A pre-stress FEA model of modal analysis based on ANSYS Mechanical is proposed. The obtained thermal stress distribution from the TES coupling analysis is transferred to this FEA model. The results are given as follows:

(1) The natural frequencies of the proposed connector are around 24.2 Hz, 75.4 Hz, 96.2 Hz and 113.6 Hz, which should be avoided in the operating condition in engineering practice.

(2) The inherent vibration is concentrated on the primary resilient bladder, which indicates that the primary bladder has a good effect on vibration attenuation. Some typical mode shapes of the primary bladder are shown in Figure 13.

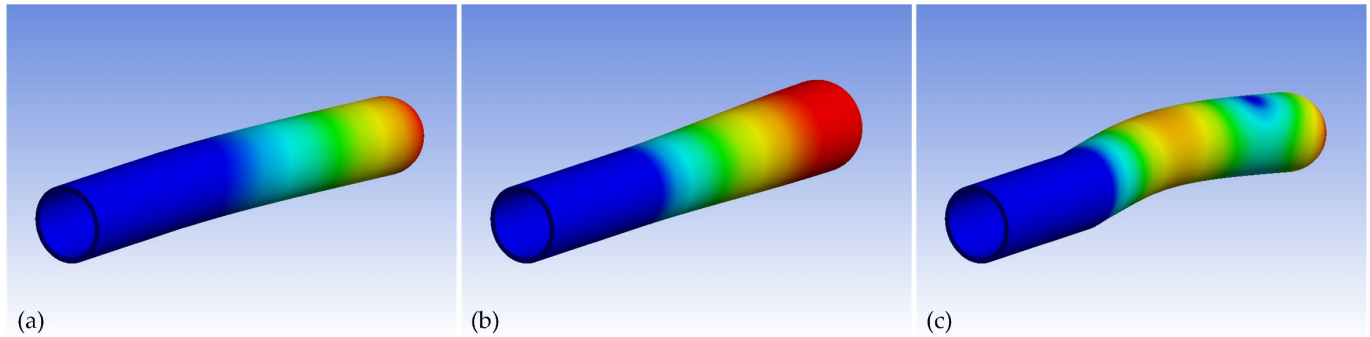


Figure 13. The mode shapes of the primary resilient bladder: (a) 1st mode, (b) 11th mode, and (c) 12th mode.

Moreover, a pre-stress FEA model of harmonic response based on ANSYS Mechanical is also proposed. The obtained thermal stress distribution from the TES coupling analysis is transferred to this FEA model, too. The frequency spacing ranges from 0 Hz to 70 Hz. Figure 14 gives the mode shape and the frequency response of the secondary resilient bladder. The results show that the harmonic response is concentrated on the secondary resilient bladder. Therefore, we can realize another advantage of the proposed dual-bladder PBOF technology; that is, the primary bladder has the function of inherent vibration attenuation, while the secondary bladder has the function of harmonic vibration attenuation.

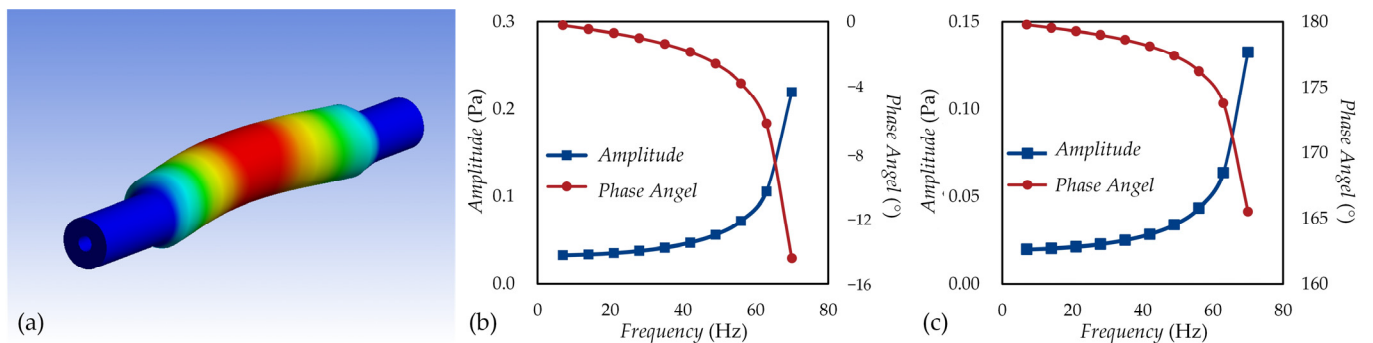


Figure 14. The harmonic response analysis of the secondary resilient bladder: (a) mode shape, (b) frequency response in the axial direction, and (c) frequency response in the radial direction.

4. Prototype and Test

4.1. Prototyping

According to the previously described design and analysis, a prototype of the proposed wet-mateable electrical connector has been manufactured. Figure 15 presents some important parts of prototyping. Because the primary resilient bladder has been developed successfully [5], four secondary resilient bladders are made of the same material by injection moulding, shown in Figure 15a. The insulating layer of the contact pin is made of PEEK also by injection moulding, shown in Figure 15b. The latching member is made of HP 7500 nylon by 3D-printing, shown in Figure 15c. Figure 15d presents four assemblies of electric contact. Figure 15e shows some custom syringes for oil-filling, in which a notch is formed in the end-face of hypodermic tubes by wire-electrode cutting. This is a cost-saving way compared with the way of manufacturing with computer numerical control (CNC). Importantly, before filling the oil, the air in the oil chambers should be extracted by the

syringe, and then, the oil with the determined volume can be injected, which is shown in Figure 15e. Finally, we complete the assembly of the prototype, which is shown in Figure 16. For the convenience of the pressure test, four electrical channels of the plug are connected in pairs (Channel I to IV, Channel II to III), and two flanges are installed to the plug and the receptacle.

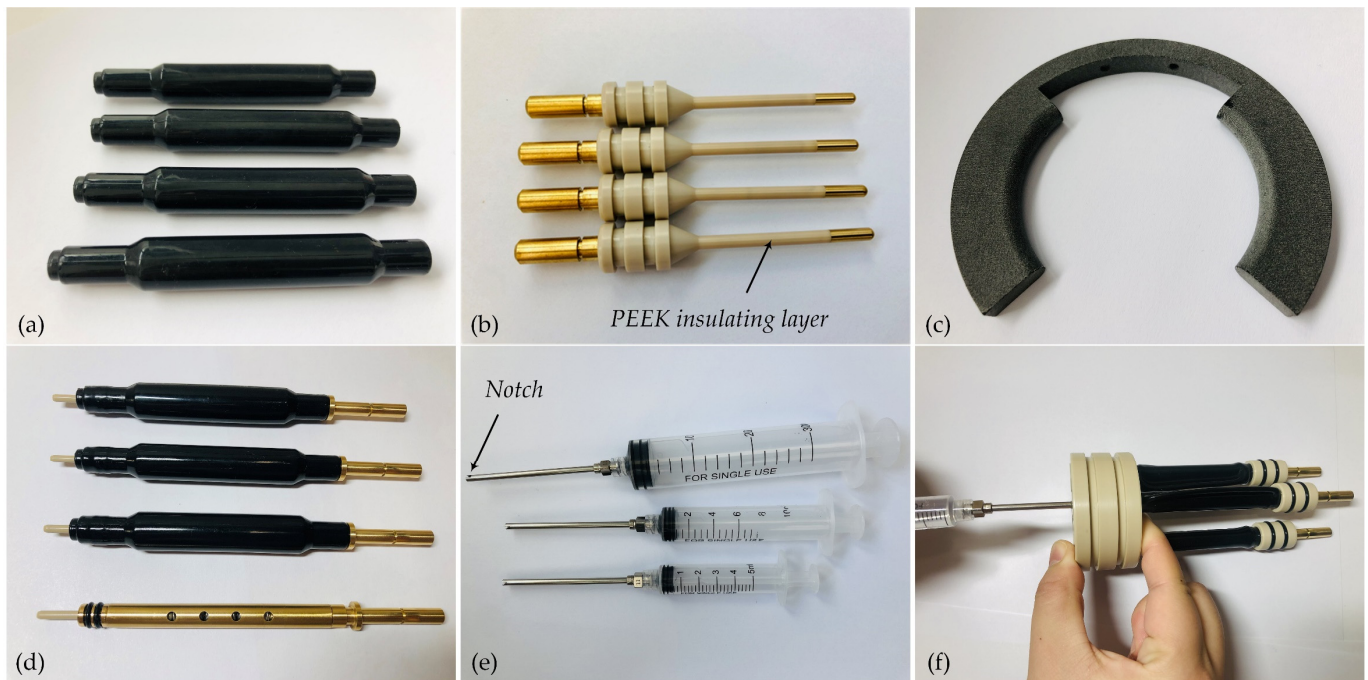


Figure 15. The core components in the prototyping of the proposed wet-mateable electrical connector: (a) secondary resilient bladders, (b) contact pins with PEEK insulating layers, (c) latching member, (d) assemblies of electric contact, (e) oil-filling syringe, (f) process of oil-filling.

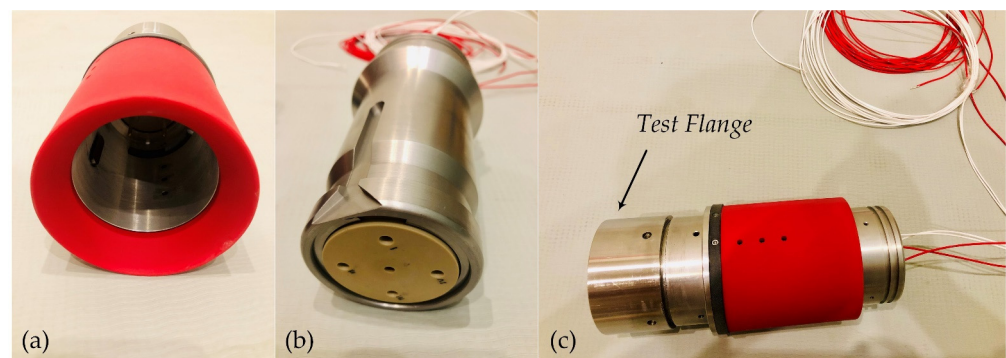


Figure 16. A prototype of the proposed wet-mateable electrical connectors: (a) the plug unit, (b) the receptacle unit, and (c) the fully-mated state of the prototype.

4.2. Electrical and Pressure Testing

The electrical performance of the prototype is qualified in accordance with the specification SEAFOM TSD-02, which is a key standard covering the requirement for designing and testing a wet-mateable connector [22]. First, the electrical performance of the prototype has been fully tested in a dry environment. The contact resistance is measured by the UNI-T® UT620C digital micro-ohm-meter with 4-wire Kelvin type measurement, and the insulation resistance is measured by the VICTOR® VC60E+ insulation tester under the voltage of 2.5 kV/DC. The results (see Table 3) show that the contact resistance is lower than 2 mΩ and the insulation resistance is above 10 GΩ, which are satisfied with the design

requirements. Also, the prototype has passed the proof voltage test of 1.0 kV/DC with the Tonghui® TH9320 hipot tester. The photos of the above tests are shown in Figure 17.

Table 3. Electrical test results of the prototype in a dry environment *.

Test Type	Contact Resistance	Insulation Resistance	Proof Voltage
Channel I	1.750 mΩ	-	-
Channel II	1.819 mΩ	-	-
Channel III	1.785 mΩ	-	-
Channel IV	1.764 mΩ	-	-
Channel I-II	-	12.78 GΩ	1.0 kV/DC
Channel III-IV	-	12.99 GΩ	1.0 kV/DC

* All the tests are performed in accordance with SEAFOM TSD-02.



Figure 17. Electrical testing of the prototype: (a) contact resistance test, (b) insulation resistance test, and (c) proof voltage test.

Then, the online test of electrical performance was conducted in a hydrostatic pressure environment, and the schematic is illustrated in Figure 18. Here, a pressure chamber in the Hadal Science and Technology Research Centre (HSTRC) of Shanghai Ocean University is used. The fully-mated prototype is installed inside the pressure chamber where four test wires are penetrated through it. The electrical performance of the prototype has been verified in the pressure environment with an ocean depth of 3000 m. Figure 19 gives the electrical performance curves of the prototype in a hydrostatic pressure environment, which shows that:

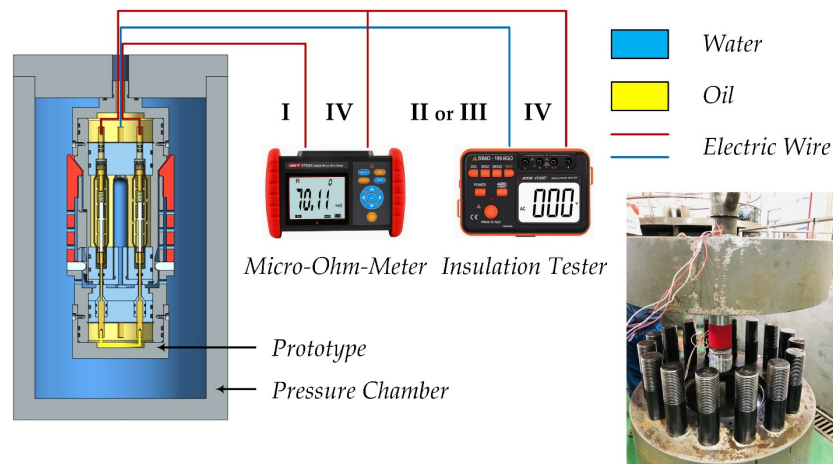


Figure 18. A schematic illustration of the prototype’s online test of electrical performance in pressure environment.

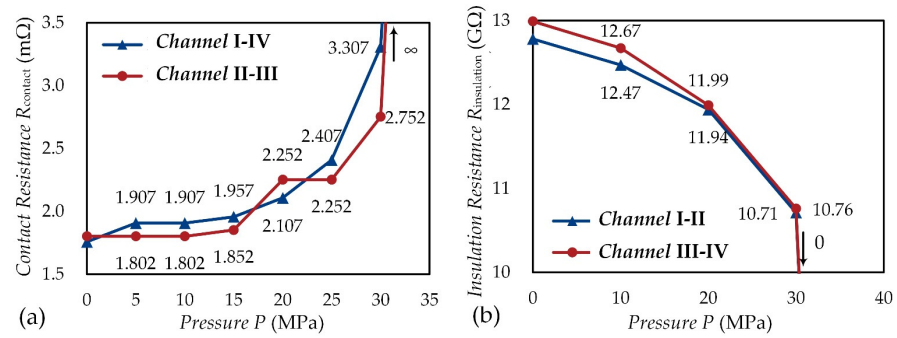


Figure 19. The electrical performance curves of the prototype in a hydrostatic pressure environment: (a) contact resistance and (b) insulation resistance.

(1) When the test pressure is less than 30 MPa, the electrical performance of the prototype can meet the design requirements. The contact resistance is about 3.3 mΩ in maximum while the insulation resistance is about 10.71 GΩ at minimum.

(2) As the test pressure increases, the contact resistance is increased while the insulation resistance is decreased. It reminds us that leakage plays a decisive role in the electrical performance of wet-mateable electrical connectors.

(3) When the test pressure exceeds 30 MPa, the differential pressure of the prototype will be higher than the sealing pressure of the O-rings used in the shuttle pin design. Thus, the failure of the penetrable self-sealing will cause a large amount of water to intrude into the electric contact, which results in infinite contact resistance and zero insulation resistance.

4.3. Failure Analysis

The above tests also revealed the failure modes of wet-mateable electrical connectors, which are discussed as follows:

(1) The main failure mode of wet-mateable connectors is sealing failure [23]. For the proposed connector, because the dual-bladder PBOF technology is introduced, only the common O-ring is used in the shuttle pin design. Additionally, its small size limits the sealing pressure of the penetrable self-sealing.

(2) Another important failure mode is the PBOF failure. Some ultimate pressure tests were conducted on the prototype. Under the condition with a very large pressure rate (about 10 MPa/min), the destruction of the primary resilient bladder was observed. As is shown in Figure 20, a very clean cut appears on the primary bladder. The PBOF failure can lead to the rapid loss of the sealing performance, which must be avoided.

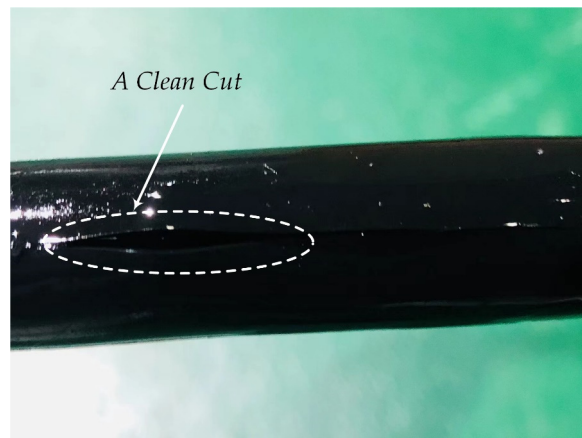


Figure 20. A destructed primary resilient bladder in the ultimate pressure test.

According to the failure analysis, we can realize how to improve the depth rate of the prototype in the future, and two aspects should be focussed on as follows:

- (1) Replace the rod seals in the shuttle pin design to improve the sealing performance of the penetrable seal-sealing. For example, O-rings made of fluorosilicone rubber with high hardness or other rod seals with high sealing pressure can be used.
- (2) Woven fabrics can be added to the material of resilient bladders to enhance the strength, which can improve the reliability of PBOF technology.

5. Discussion and Conclusions

This paper presents a methodology for designing and testing a wet-mateable electrical connector, which might be the first discloser on this topic in the aspects of design, theory, simulation and testing. The innovations of the proposed connector can be summarized as follows:

(1) The dual-bladder PBOF design used in the proposed connector is mainly based on the low-cost primary resilient bladder, which is different from some COTS products' designs (e.g., SECAON HydraElectric, NautilusTM WM1.7-30 and Siemens DigiTRON). The bladders used in COTS products are often very large, which are usually very difficult to manufacture by injection moulding.

(2) The AID design used in the proposed connector is also different from what is used in NautilusTM WM1.7-30 and Siemens DigiTRON. Also, the latching member can be made directly by 3D printing, which is cost-effective.

(3) In fact, the cost of developing a wet-mateable connector is very high. We have almost reached the limit of cost control in the R&D process. From another perspective, with lower cost and a shorter development cycle, we have made some major breakthroughs in this bottleneck field in China, and this benefited from the previous review research and the use of innovative simulation techniques.

It should be noted that the wet-mating online test of electrical performance in a high-pressure environment has not been carried out in this paper. To realize the wet-mating operation in a high-pressure environment, a specially-customized pressure chamber should be required. Unfortunately, such equipment is unavailable to us at present, which also involves a lot of key technologies. Limited by our financial conditions, the depth rate of the prototype and the test condition can only reach the present level, which can be improved in the future.

The main conclusions can be summarized as follows:

(1) An innovative wet-mateable connector has been proposed, which involves the dual-bladder PBOF technology, the penetrable self-sealing design, and the AID technology.

(2) The generalized differential pressure equations of the dual-bladder PBOF technology have been derived. The results show that the differential pressure provided by the bladder under the action of internal pressure is much larger than that provided by such a bladder with a similar dimension but under the action of external pressure.

(3) A procedure of thermal-electric-structure (TES) coupling simulation for wet-mateable electrical connectors has been proposed, and a series of FEA involving coupled multi-field problems have been conducted, including thermal-electric coupling analysis, static structural analysis, and dynamic analysis. The results show that the underwater environment allows better heat dissipation of wet-mateable electrical connectors, which can further be improved by the dual-bladder PBOF technology. Also, the primary resilient bladder has the function of inherent vibration attenuation while the secondary resilient bladder has the function of harmonic vibration attenuation.

(4) A prototype of the proposed connector has been developed successfully, and many process problems of core components have been solved. The electrical performance of the prototype has been verified by the online test in the hydrostatic pressure environment with an ocean depth of 3000 m. The technical level has reached the leading position in China.

(5) The failure modes of wet-mateable connectors have been revealed, mainly including the sealing failure and the PBOF failure. The rod seals with high sealing pressure should

be used in the shuttle pin design. The woven fabric-reinforced fluorosilicone rubber can be used to make resilient bladders to improve the reliability of PBOF technology. Additionally, the glass fibre-reinforced PEEK can be used to provide better resistance to dielectric breakdown.

Author Contributions: Conceptualization, W.S., C.Y., W.C., C.S., J.H. and Y.L.; methodology, W.S., W.C., C.S., P.Y., J.H., Y.L., Q.L. and Z.W.; software, W.S. and Z.W.; validation, W.C.; formal analysis, W.S.; investigation, W.S., C.Y., J.H. and Y.L.; resources, W.S., C.Y., W.C., C.S., P.Y., Y.L. and Q.L.; data curation, W.S. and W.C.; writing—original draft preparation, W.S.; writing—review and editing, W.S. and W.C.; visualization, W.S.; supervision, C.Y. and W.C.; project administration, C.Y. and W.C.; funding acquisition, C.Y., W.C., C.S. and P.Y. All authors have read and agreed to the published version of the manuscript.

Funding: This work was supported by Zhejiang Key R&D Program of China (Grant No. 2021C03157), the Startup funding of New-Joined PI of Westlake University (Grant No. 041030150118), and the Scientific Research Funding Project of Westlake University (Grant No. 2021WUFP017).

Institutional Review Board Statement: Not applicable.

Informed Consent Statement: A Not applicable.

Data Availability Statement: Not applicable.

Acknowledgments: We also would like to thank the colleagues of Hadal Science and Technology Research Centre (HSTRC) of Shanghai Ocean University.

Conflicts of Interest: The authors declare no conflict of interest.

References

- Borthwick, A.G.L. Marine renewable energy seascape. *Engineering* **2016**, *2*, 69–78. [CrossRef]
- Song, W.T.; Cui, W.C. Review of deep-ocean high-pressure simulation systems. *Mar. Technol. Soc. J.* **2020**, *54*, 68–84. [CrossRef]
- Song, W.T.; Cui, W.C. An overview of underwater connectors. *J. Mar. Sci. Eng.* **2021**, *9*, 813. [CrossRef]
- Menandro, P.S.; Bastos, A.C. Seabed mapping: A brief history from meaningful words. *Geosciences* **2020**, *10*, 273. [CrossRef]
- Song, W.T.; Yang, C.B.; Cui, W.C.; Lei, Y.; Hong, J.; Wang, Z.H.; Hu, Z.Y. Study of pressure-balanced oil-filled (PBOF) technology. *Ocean Eng.* **2022**, *260*, 111757. [CrossRef]
- Collin, A.J.; Nambiar, A.J.; Bould, D.; Whitby, B.; Moonem, M.A.; Schenkman, B.; Atcity, S.; Chainho, P.; Kiprakis, A.E. Electrical components for marine renewable energy arrays: A techno-economic review. *Energies* **2017**, *10*, 1973. [CrossRef]
- Rémouit, F.; Ruiz-Minguela, P.; Engström, J. Review of electrical connectors for underwater applications. *IEEE J. Ocean. Eng.* **2018**, *43*, 1037–1047. [CrossRef]
- Wood Group Kenny. *Wet Mate Connector Market Study*; Technical Report 2500014-01-D-3-001; ORE Catapult: Glasgow, UK, 2014; Available online: <https://ore.catapult.org.uk/wp-content/uploads/2018/01/Wet-mate-connector-study.pdf> (accessed on 13 December 2022).
- Weiss, P.; Beurthey, S.; Chardard, Y.; Dhedin, J.F.; Andre, T.; Rabushka, K.; Tourcher, C.; Gauch, F.; Micoli, C. Novel wet-mate connectors for high voltage and power transmissions of ocean renewable energy systems. In Proceedings of the 4th International Conference on Ocean Energy 2012, Dublin, Ireland, 17–19 October 2012; ICOE: Lisbon, Portugal, 2022. Available online: https://www.icoe-conference.com/publication/novel_wet_mate_connectors_for_high_voltage_and_power_transmissions_of_ocean_renewable_energy_systems/ (accessed on 13 December 2022).
- ANTARES Collaboration. ANTARES: The first undersea neutrino telescope. *Nucl. Instrum. Methods A* **2011**, *656*, 11–38. [CrossRef]
- KM3NeT Collaboration. Deep-sea deployment of the KM3NeT neutrino telescope detection units by self-unrolling. *J. Instrum.* **2020**, *15*, P11027. [CrossRef]
- Han, Q.; Chen, H.Y.; Yang, W.C.; Zhang, Y.; Yang, J.K.; Chen, Y.F. Analysis of reciprocating O-ring seal in the pressure-balanced oil-filled wet-mate electrical connectors for underwater applications. *Lubr. Sci.* **2019**, *31*, 335–345. [CrossRef]
- Song, W.T.; Cui, W.C. Design of a practical metal-made cold isostatic pressing (CIP) chamber using finite element analysis. *Materials* **2022**, *15*, 3621. [CrossRef]
- Antonova, E.E.; Looman, D.C. Finite elements for thermoelectric device analysis in ANSYS. In Proceedings of the ICT 2005 24th International Conference on Thermoelectrics, Clemson, CA, USA, 19–23 June 2005; IEEE: New York, NY, USA, 2015; pp. 215–218. [CrossRef]
- Sun, B.A.; Li, W.K.; Wang, Z.H.; Zhu, Y.P.; He, Q.; Guan, X.Y.; Dai, G.M.; Yuan, D.H.; Li, A.; Cui, W.C.; et al. Recent progress in modelling and control of bio-inspired fish robots. *J. Mar. Sci. Eng.* **2022**, *10*, 773. [CrossRef]
- Liu, Q.M.; Chen, H.; Wang, Z.H.; He, Q.; Chen, L.K.; Li, W.K.; Li, R.P.; Cui, W.C. A manta ray robot with soft material based flapping wing. *J. Mar. Sci. Eng.* **2022**, *10*, 962. [CrossRef]

17. Lin, M.L.; Lin, R.; Yang, C.J.; Li, D.J.; Zhang, Z.Y.; Zhao, Y.C.; Ding, W.J. Docking to an underwater suspended charging station: Systematic design and experimental test. *Ocean Eng.* **2022**, *249*, 110766. [[CrossRef](#)]
18. Fan, F.H.; Ishibashi, S. Underwater applications of light emitting diodes. In Proceedings of the 2015 IEEE Underwater Technology (UT), Chennai, India, 23–25 February 2015; IEEE: New York, NY, USA, 2015; p. 15143567. [[CrossRef](#)]
19. Song, W.T.; Cui, W.C. Underwater Wet Plugging Electric Connector Capable of Realizing Pressure Equilibrium. China Patent CN 112600029 B, 29 October 2021.
20. Cairns, J.L. Spark-Proof Hostile Environment Connector. U.S. Patent 5,194,012, 16 March 1993.
21. Thongsri, J. Transient thermal-electric simulation and experiment of heat transfer in welding tip for reflow soldering process. *Math. Probl. Eng.* **2018**, *2018*, 4539054. [[CrossRef](#)]
22. SEAFOM. Functional Design and Test Specification for Subsea Electrical and Optical Connectors and Jumpers; SEAFOM TSD-02; Epsom, UK, 2016. 2016. Available online: <https://seafom.com/?mdocs-file=78> (accessed on 13 December 2022).
23. Lamare, P.; Vernin, P. Underwater mateable electro-optical connectors: The feedback from ANTARES. *Nucl. Instrum. Meth. A* **2009**, *602*, 252–254. [[CrossRef](#)]

Disclaimer/Publisher’s Note: The statements, opinions and data contained in all publications are solely those of the individual author(s) and contributor(s) and not of MDPI and/or the editor(s). MDPI and/or the editor(s) disclaim responsibility for any injury to people or property resulting from any ideas, methods, instructions or products referred to in the content.